Hindawi
Wireless Communications and Mobile Computing
Volume 2021, Article ID 9979881, 9 pages
https://doi.org/10.1155/2021/9979881

Research Article

DOA Estimation with Spatial Spread Vector-Sensor Array Based on Biquaternion MUSIC

Qinyu Zhu,[1,2] **Guimei Zheng**,[2] **Chen Chen**,[1,2] **and Qian Guo**[1,2]

[1]*Postgraduate School, Air Force Engineering University, Xi'an 710038, China*
[2]*Air and Missile Defense College, Air Force Engineering University, Xi'an 710038, China*

Correspondence should be addressed to Guimei Zheng; zheng-gm@163.com

Received 21 March 2021; Revised 30 July 2021; Accepted 5 August 2021; Published 17 August 2021

Academic Editor: Abdul Basit

The mutual coupling among various components of the collocated crossdipole (CCD) vector-sensor is severe, and its application is greatly limited. The spatial spread dipole (SSD) vector-sensor can avoid this problem, but the multiple signal classification (MUSIC) algorithm for the SSD array is rarely developed. In view of this situation, this paper proposed a MUSIC-like algorithm for the SSD array. The biquaternion model was first established, and the biquaternion MUSIC (BQ-MUSIC) algorithm was developed on the basis of this model, for the two-dimensional direction-of-arrival (2D-DOA) estimation. Our proposed algorithm requires low computational complexity by adopting the dimensionality reduction method. Numerical simulations verify the effectiveness of the proposed algorithm.

1. Introduction

The electromagnetic vector-sensor (EMVS) array is also known as polarization sensitive array due to their ability to sense the polarization information of electromagnetic waves. Compared with traditional scalar array, EMVS array can obtain more information in the time domain and frequency domain such as phase and frequency waveforms, with stronger anti-interference ability, higher spatial resolution, and better detection robustness ability [1]. EMVS array also has the following advantages: (1) they can sense electromagnetic waves in a vector mode and provide polarization information of electromagnetic sources; (2) collocated EMVS that appeared in the early stage is suitable for the direction of arrival estimation for near-field or far-field, broad-band, or narrow-band signals; (3) different polarization information can be exploited in polarization domain when polarization electromagnetic wave cannot be distinguished in the spatial domain. Meanwhile, the appropriate application of polarization diversity technology could bring great convenience to the subsequent target recognition and classification; (4) when the spatial aperture of the array is small, the EMVS array still have a better resolution. Therefore, it is suitable for limited physical space such as mobile platform [2]. EMVS array has become a research hotspot in the field of array signal processing and is widely used in sonar radar communications.

Direction-of-arrival (DOA) estimation represents a vital research direction of array signal processing. Based on previous researches on DOA estimation method for scalar array, scholars have transplanted and applied MUSIC [3], estimated signal parameters via rotational invariance techniques (ESPRIT) [4], and maximum likelihood (ML) [5] to vector-sensor array signal processing, and achieved favorable estimation results. Particularly, some studies have used the Poynting vector crossproduct relationship that only the vector-sensor can perceive. However, the time-domain ESPRIT algorithm developed based on this relationship has high requirements on the source, thus limiting the application scenarios [6, 7]. Polarization smoothing is used to realize the DOA estimation of coherent sources by using the method of dephasing intervention processing [8]. On the other hand, this method is suitable for all array structures and does not lose the effective aperture of the array compared with spatial smoothness [9].

In the long vector (LV) model, multiple components of each antenna are directly "stacked" into a column vector,

and this representation has the advantages of simplicity and manipulation. However, the orthogonal relationship among the components of each array element is lost at the same time. The hypercomplex number as typified by quaternion is very suitable for the component representation of EMVS because of its strict orthogonality [10]. With the breakthrough of some mathematical problems such as the eigenvalue decomposition (EVD) of the quaternion value matrix [11], the hypercomplex number tool has been introduced into the research of EMVS array signal processing successfully [10–16]. The frequency-domain quaternion MUSIC algorithm [12] and frequency-domain biquaternion MUSIC algorithm [13] are explored, respectively. Even though the two algorithms can simultaneously estimate direction parameters and polarization parameters, they require a four-dimensional (4-D) spectral peak search at the very least, which brings enormous computing burdens. Li et al. have proposed a Q-MUSIC algorithm that can realize dimensionality reduction search on the premise of excluding only a few special parameters in the time domain [14]. Correspondingly, quaternion ESPRIT [15, 16] and augment ESPRIT [17] algorithms have also been developed.

Most of the studies mentioned above [3–6, 8–16] mainly focus on collocated vector-sensor array. In actual production, this collocated EMVS with the same geometric center requires high degree of electromagnetic isolation. As the frequency increases, the cost of implementation will go up. Therefore, some scholars have studied the noncollocated EMVS. According to the modified vector crossproduct method based on the ingenious array arrangement, Wong et al. [18] have obtained a 2-D DOA estimation of the spatially spread vector-sensors. Spatial ESPIRT [19] was developed by Zheng based on Ref. [7]. Then, by combining the coarse and fine estimations, the high-accuracy 2-D DOA estimation can be obtained. Gong et al. have put forward a spatially spread quint of dipoles or loops that are symmetrical in space. With this feature, an efficient DOA and polarization estimator is realized using the vector crossproduct method [20].

However, the introduction of the spatial phase shift factor inside the sensor makes LV-MUSIC dimensionality reduction difficult to be realized, and the 4-D search poses unacceptable calculation burdens. Therefore, most DOA estimation algorithms for SSD array are based on ESPRIT-like. In this paper, we first introduce the biquaternion operation and EVD of its Hermitian matrix and then create a high-dimensional algebraic model of the SSD-EMVS array that has a very compact form. The characteristics of the approximation of the covariance matrix of CCD array and SSD array are illustrated. The resulting BQ-MUSIC algorithm is developed to easily achieve dimensionality reduction, with promising results. Finally, we use simulation experiments to verify the effectiveness of the proposed algorithm.

2. Biquaternion Operation and EVD of Hermitian Matrix

Notation: $\mathbb{R}$, $\mathbb{C}$, $\mathbb{C}$, and $\mathbb{H}_{\mathbb{C}}$ represent real numbers, complex numbers, quaternion numbers, and biquaternion numbers, respectively. $\mathbb{C}_1$ marks the complex numbers with the imaginary part of I and $I^2 = -1$. "†" stands for quaternion or biquaternion conjugate transpose; "^{H}" refers to complex conjugate transpose; "*" is the complex conjugate.

Quaternion, as a kind of high-dimensional complex number, has one real component and three imaginary components. By extending the real number coefficients of each component in quaternions to the complex number, the biquaternions (also known as complexified quaternions) are obtained. And a biquaternion $q \in \mathbb{H}_{\mathbb{C}}$ is defined as

$$q = q_0 + q_1 i + q_2 j + q_3 k, \tag{1}$$

where $q_0, q_1, q_2, q_3 \in \mathbb{C}_1$. The multiplications among the three imaginary units $i, j, k$of a biquaternion characterizing the orthogonality relation are not commutative, but the multiplication between the complex imaginary unit I and the quaternion imaginary i, j, k units satisfied the commutative law [10]. The following standard relations among all imaginary units (quaternion and complex) hold

$$\begin{gathered} iI = Ii, jI = Ij, kI = Ik, \\ i^2 = j^2 = k^2 = ijk = -1, \\ ij = -ji = k, jk = -kj = i, \\ ki = -ik = j. \end{gathered} \tag{2}$$

Biquaternion, as an extension of quaternion, also can be written in the form of the sum of real and imaginary parts, but the coefficients of each part are all complex values, shown as follows:

$$q = \mathcal{S}(q) + \mathcal{V}(q), \tag{3}$$

where

$$\begin{cases} \mathcal{S}(q) = q_0, \\ \mathcal{V}(q) = q_1 i + q_2 j + q_3 k. \end{cases} \tag{4}$$

The conjugate of a $q \in \mathbb{H}_{\mathbb{C}}$, noted $q^\dagger$, is given by

$$q^\dagger = q_0^* - q_1^* i - q_2^* j - q_3^* k. \tag{5}$$

And the norm of q, noted $|q|$, is given by

$$|q| = \sqrt{|q_0|^2 + |q_1|^2 + |q_2|^2 + |q_3|^2}. \tag{6}$$

It should be noted that $\forall q \in \mathbb{H}_{\mathbb{C}}$, $|q| \geq 0$, and $|q| = 0 \Rightarrow q = 0$.

A biquaternion value matrix $\mathbf{B} \in \mathbb{H}_{\mathbb{C}}^{m\times n}$ can be rewritten as $\mathbf{B} = \mathbf{B}_1 + I\mathbf{B}_2$, where $\mathbf{B}_1, \mathbf{B}_2 \in \mathbb{H}^{m\times n}$. Usually, EVD operation on the high-dimensional algebraic matrix is realized by its isomorphic adjoint matrix. The adjoint matrix of $\mathbf{B}$ is

recorded as $\Upsilon_{\mathbf{B}} \in \mathbb{H}^{2m\times 2n}$, and

$$\Upsilon_{\mathbf{B}} = \begin{pmatrix} \mathbf{B}_1 & \mathbf{B}_2 \\ -\mathbf{B}_2 & \mathbf{B}_1 \end{pmatrix}. \tag{7}$$

Particularly, if $\mathbf{B}$ is a Hermitian matrix, then $\Upsilon_{\mathbf{B}}$ is a Hermitian matrix. Then, $\Upsilon_{\mathbf{B}}$ has the following quaternion value matrix EVD: $\Upsilon_{\mathbf{B}} = \mathbf{UDU}^{\dagger}$, where $\mathbf{U} \in \mathbb{H}^{2n\times 2n}$ and $\mathbf{D} \in \mathbb{R}^{2n\times 2n}$. According to the "isomorphism" property, the eigenvalues of $\mathbf{B}$ and $\Upsilon_{\mathbf{B}}$ are the same (both results are in $\mathbf{D}$), and $\mathbf{U}_b \in \mathbb{H}_{\mathbb{C}}^{n\times 2n}$ contains the eigenvectors of $\mathbf{B}$ on its columns, as shown in

$$\mathbf{U}_b = \frac{1}{\sqrt{2}}\mathbf{\Psi}_n\mathbf{U}, \tag{8}$$

where $\mathbf{\Psi}_n \in \mathbb{C}_I^{n\times 2n}$, $\mathbf{\Psi}_n = (\mathbf{I}_n, -I\mathbf{I}_n)$, and I_n are the $n \times n$ unit matrix. Finally, we obtain the EVD of a biquaternion valued matrix:

$$\mathbf{B} = \mathbf{U}_b\mathbf{D}\mathbf{U}_b^{\dagger}. \tag{9}$$

3. Array Signal Model

A collocated crossed dipole electromagnetic vector-sensor (CCD EMVS) is shown in Figure 1 and consists of three electric dipoles, namely, E_x, E_y, E_z. The output of each component is e_x, e_y, e_z, respectively, and the value are [1]

$$\begin{cases} e_x = \cos\theta\cos\varphi\sin\gamma e^{I\eta} - \sin\varphi\cos\gamma, \\ e_y = \cos\theta\sin\varphi\sin\gamma e^{I\eta} + \cos\varphi\cos\gamma, \\ e_z = -\sin\theta\sin\gamma e^{I\eta}, \end{cases} \tag{10}$$

where (θ, φ) and (γ, η) are the elevation-azimuth 2D-DOA (labeled in Figure 1) and polarization of an electromagnetic wave, respectively, and $\theta \in [0, \pi]$, $\varphi \in [0, 2\pi)$, $\gamma \in [0, \pi/2]$, and $\eta \in [-\pi, \pi]$. The output of the EMVS, as a whole, is expressed as biquaternion scalar $\xi_1(\theta, \varphi, \gamma, \eta) \in \mathbb{H}_{\mathbb{C}}$,

$$\xi_1(\theta, \varphi, \gamma, \eta) = i \cdot e_x + j \cdot e_y + k \cdot e_z. \tag{11}$$

Since its real part coefficient is zero, it is also called a pure quaternion. Compared with LV-models, this pure biquaternion representation method is not only more compact in structure but also preserves orthogonality among its components.

The spatial spread dipole electromagnetic vector-sensor (SSD-EMVS) is physically isolated by translating them to a certain distance $d(d_x, d_y, d_z)$ along its respective coordinate axes. In particular, SDD-EMVS is uniform when $d_x = d_y = d_z$. The spatial phase shift factor should be introduced subsequently with d. In the SSD-EMVS, as shown in Figure 2, the spatial phase shift factors on the three components along the x, y, z-axis are $e^{-I(2\pi/\lambda)d_x\cos\theta\sin\varphi}$, $e^{-I(2\pi/\lambda)d_y\sin\theta\sin\varphi}$, and $e^{-I(2\pi/\lambda)d_z\cos\theta}$ in order [18]. Thus, the polarization response

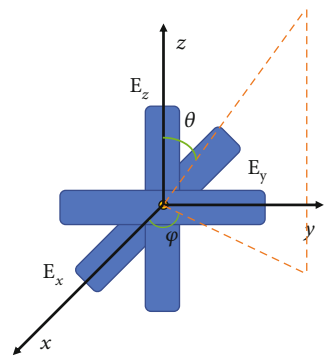

Figure 1: The structure of CCD vector-sensor.

of this vector-sensor is expressed by applying phase shift factor and a biquaternion scalar as

$$\xi(\theta, \varphi, \gamma, \eta) = i \cdot e^{-I\frac{2\pi}{\lambda}d_x\cos\theta\sin\varphi}e_x + j \cdot e^{-I\frac{2\pi}{\lambda}d_y\sin\theta\sin\varphi}e_y + k \cdot e^{-I\frac{2\pi}{\lambda}d_z\cos\theta}e_z, \tag{12}$$

where $\xi(\theta, \varphi, \gamma, \eta) \in \mathbb{H}_{\mathbb{C}}$, and λ is the wavelength of electromagnetic waves.

Consider a planar array consisting of SSD-EMVS with the first sensor position located at the origin of the coordinates, as displayed in Figure 3. M array elements are placed along the x-axis, and the spacing between two adjacent array elements is D_x. N elements are placed along the y-axis, and the spacing between two adjacent array elements is D_y.The single-column steering vector along the x-axis in this planar array is $\mathbf{q}_x \in \mathbb{C}_I^{M\times 1}$, and

$$\mathbf{q}_x = \left[1, e^{-I\frac{2\pi}{\lambda}D_x\sin\theta\cos\varphi}, \cdots, e^{-I\frac{2\pi}{\lambda}(M-1)D_x\sin\theta\cos\varphi}\right]^T. \tag{13}$$

The single-row steering vector along the y-axis in this planar array is $\mathbf{q}_y \in \mathbb{C}_I^{N\times 1}$, and

$$\mathbf{q}_y = \left[1, e^{-I\frac{2\pi}{\lambda}D_y\sin\theta\sin\varphi}, \cdots, e^{-I\frac{2\pi}{\lambda}(M-1)D_y\sin\theta\sin\varphi}\right]^T. \tag{14}$$

Hence, the spatial polarization steering vector of this polarization sensitive array is

$$\mathbf{a}(\theta, \varphi, \gamma, \eta) = \mathbf{q}(\theta, \varphi) \cdot \xi(\theta, \varphi, \gamma, \eta), \tag{15}$$

where $\mathbf{q}(\theta, \varphi) \in \mathbb{C}_I^{M\times N}$, $\mathbf{q}(\theta, \varphi) = \mathbf{q}_x \otimes \mathbf{q}_y$, and $\mathbf{a}(\theta, \varphi, \gamma, \eta) \in \mathbb{H}_{\mathbb{C}}^{MN\times 1}$, and " $\otimes$ " is the Kronecker product.

Assuming that there are L incoherent far-field fully polarized narrow-band plane waves impinge on this array, then the output of such an array is $\mathbf{X}(t) \in \mathbb{H}_{\mathbb{C}}$:

$$\mathbf{X}(t) = \sum_{l=1}^{L}\mathbf{q}(\theta_l, \varphi_l)\xi(\theta_l, \varphi_l, \gamma_l, \eta_l)s_l(t) + \mathbf{N}(t) = \mathbf{Q\Phi S} + \mathbf{N}(t) = \mathbf{AS} + \mathbf{N}(t), \tag{16}$$

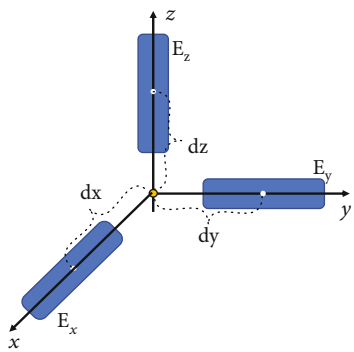

FIGURE 2: The structure of SSD vector-sensor.

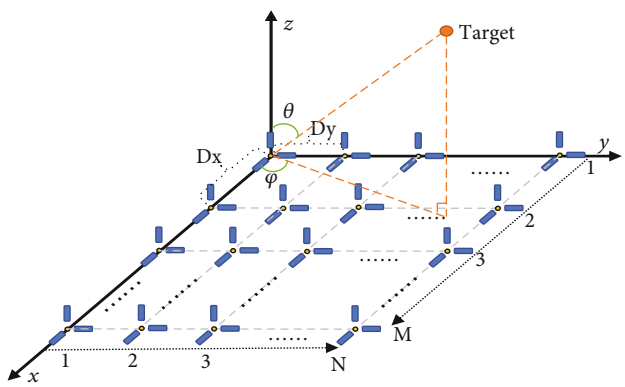

FIGURE 3: SDD-EMVS planar array geometry.

where $\mathbf{\Phi} \in \mathbb{H}_{\mathbb{C}}^{L\times L}$ is a diagonal matrix composed of $\xi(\theta_l, \varphi_l, \gamma_l, \eta_l)$ and $l = 1, 2, \cdots, L$. $\mathbf{Q} \in \mathbb{C}_I^{M\times N}$ is the spatial steering vectors matrix of this array, and $\mathbf{Q} = [\mathbf{q}(\theta_l, \varphi_l), \mathbf{q}(\theta_2, \varphi_2), \cdots, \mathbf{q}(\theta_l, \varphi_l)]$. $\mathbf{s}(t) \in \mathbb{C}_I^{L\times 1}$ is a signal vector composed of L signals, and $\mathbf{s}(t) = [s_1(t), s_2(t), \cdots, s_L(t)]^T$. The manifold of this polarization sensitive array is $\mathbf{A} \in \mathbb{H}_{\mathbb{C}}^{MN\times 1}$, and $\mathbf{A} = \mathbf{Q\Phi} = [\mathbf{a}(\theta_1, \varphi_1, \gamma_1, \eta_1), \cdots, \mathbf{a}(\theta_L, \varphi_L, \gamma_L, \eta_L)]$.

The noise data received by the nth vector-sensor of the mth row is expressed by a pure biquaternion $\mathrm{n}_{(n,m)} \in \mathbb{H}_{\mathbb{C}}$, as follows:

$$\mathrm{n}_{(n,m)} = i \cdot \mathrm{n}_{(n,m)x} + j \cdot \mathrm{n}_{(n,m)y} + k \cdot \mathrm{n}_{(n,m)z}, \tag{17}$$

where $\mathrm{n}_{(n,m)x}$, $\mathrm{n}_{(n,m)y}$, and $\mathrm{n}_{(n,m)z}$ are the noise data received by the E_x, E_y, E_z. Correspondingly, $\mathbf{N}(\mathbf{t}) \in \mathbb{H}_{\mathbb{C}}^{MN\times 1}$ is the noise vector formed by the noise data received by $M \times N$ array elements in the biquaternion model.

4. Biquaternion-MUSIC for SSD Array

Under the above signal model, the data covariance matrix $\mathbf{R}_X \in \mathbb{H}_{\mathbb{C}}^{MN\times MN}$ is calculated by

$$\mathbf{R}_X = E\left[\mathbf{X}(t)\mathbf{X}^{\dagger}(t)\right] = \mathbf{QZQ}^H + \mathbf{R}_{\mathbf{N}}, \tag{18}$$

$$\mathbf{Z} = E\left(\mathbf{\Phi SS}^H\mathbf{\Phi}^{\dagger}\right) = \mathbf{\Phi R}_S\mathbf{\Phi}^{\dagger}. \tag{19}$$

Since the signal sources are assumed to be incoherent, the signal covariance matrix $\mathbf{R}_S$ is a diagonal matrix. And the multiplications between two diagonal matrices can be exchanged with each other. $\mathbf{Z}$ can be rewritten as

$$\mathbf{Z} = \mathbf{R}_S\mathbf{\Phi\Phi}^{\dagger}, \tag{20}$$

$\mathbf{\Phi\Phi}^{\dagger} = \mathrm{diag}\ \{|\xi(\theta_1, \varphi_1, \gamma_1, \eta_1)|^2, \cdots, |\xi(\theta_l, \varphi_l, \gamma_l, \eta_l)^2|\}$.

Considering a quaternion model for the collocated double electric dipoles array, its polarization response scalar is$\zeta_1 \in \mathbb{H}$, and

$$|\zeta_1|^2 = \zeta_1\zeta_1^{\dagger}, \tag{21}$$

where $|\zeta_1|^2 \in \mathbb{R}$. For spatial spread vector-sensor of the same type, the product of its polarization response scalar is $\zeta \in \mathbb{H}$, and

$$|\zeta|^2 = \zeta\zeta^{\dagger}. \tag{22}$$

Its norm of all internal spatial phase shift factors is 1; so, $|\zeta_1|^2 = |\zeta|^2$. Finally, we have a conclusion that in the quaternion model established for the double electric dipole array, the covariance matrix is the same regardless of whether it is collocated or spatial spread (the process analogy from Eq. (18) to Eq. (20)).

Unfortunately, equation $|\xi|^2 = \xi\xi^{\dagger}$ does not hold the biquaternion operation anymore. In fact, it can be inferred from Eq. (6) that

$$\xi\xi^{\dagger} = \mathscr{S}\left(\xi\xi^{\dagger}\right) + \mathscr{V}\left(\xi\xi^{\dagger}\right) = \left|\xi\xi^{\dagger}\right|^2 + \mathscr{V}\left(\xi\xi^{\dagger}\right). \tag{23}$$

For the CCD vector-sensor, there is

$$\xi_1\xi_1^{\dagger} = \mathscr{S}\left(\xi_1\xi_1^{\dagger}\right) + \mathscr{V}\left(\xi_1\xi_1^{\dagger}\right) = \left|\xi_1\xi_1^{\dagger}\right|^2 + \mathscr{V}\left(\xi_1\xi_1^{\dagger}\right). \tag{24}$$

Since $|\xi\xi^{\dagger}|^2 = |\xi_1\xi_1^{\dagger}|^2$ and $\mathscr{V}(\xi\xi^{\dagger}) \neq \mathscr{V}(\xi_1\xi_1^{\dagger})$, it is clearly that $\xi\xi^{\dagger} \neq \xi_1\xi_1^{\dagger}$, which directly leads to the $\mathbf{R}_X$ of SDD-EMVS that is different from its collocated counterpart one, unlike the quaternion model.

However, thanks to the exponential form of the phase shift factor and the feature that the real part of the pure biquaternion is 0, the difference between the $\xi\xi^{\dagger}$ and $\xi_1\xi_1^{\dagger}$ can be quantified by err,

$$\mathrm{err} = \frac{\left|\xi\xi^{\dagger}\text{-}\xi_1\xi_1^{\dagger}\right|}{\left|\xi_1\xi_1^{\dagger}\right|} = \frac{\left|\mathscr{V}\left(\xi\xi^{\dagger}\right) - \mathscr{V}\left(\xi_1\xi_1^{\dagger}\right)\right|}{\left|\xi_1\xi_1^{\dagger}\right|}. \tag{25}$$

We perform 1000 independent experiments under different $|\xi|$ and draw the different curves of $|\xi_1\xi_1^{\dagger}|$ and $|\xi\xi^{\dagger}|$ in Figure 4. As can be seen in Figure 4, err is always around 0.05 when $|\xi|$ goes from 10^{-4} to 1, and then err decreases as $|\xi|$ increases. The small difference between $\xi\xi^{\dagger}$ and $\xi_1\xi_1^{\dagger}$ eventually leads to that the $\mathbf{R}_X$ of SSD-EMVS array, and $\mathbf{R}_{X1}$ of

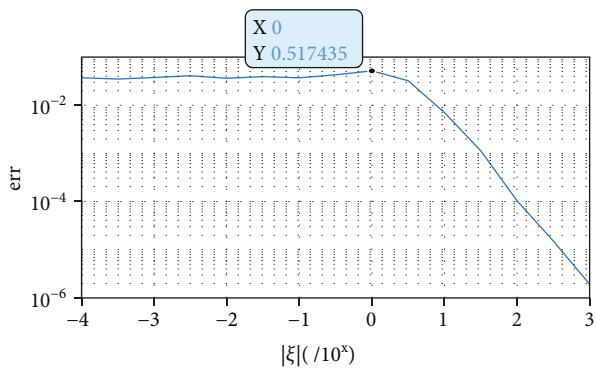

Figure 4: The difference between $\xi\xi^{\dagger}$ and $\xi_1\xi_1^{\dagger}$.

collocated vector-sensor array is exactly the same in real part and only slightly different in the imaginary parts.

The EVD of $\mathbf{R}_X$ by Eqs. (7)–(9) has

$$\mathbf{R}_X = \mathbf{U}_S\mathbf{D}_S\mathbf{U}_S^{\dagger} + \mathbf{U}_N\mathbf{D}_N\mathbf{U}_N^{\dagger}, \tag{26}$$

where $\mathbf{U}_S \in \mathbb{H}_{\mathbb{C}}^{MN\times 2L}$ is the biquaternion-value signal subspace matrix corresponding to large eigenvalues matrix $\mathbf{D}_S$, and $\mathbf{U}_N \in \mathbb{H}_{\mathbb{C}}^{MN\times 2(MN-L)}$ is the biquaternion-value noise subspace corresponding to small eigenvalues matrix $\mathbf{D}_N$. According to the subspace theory, the signal subspace $\mathbf{U}_S$ and the noise subspace $\mathbf{U}_N$ are orthogonal to each other as in complex-value matrix and quaternion-valued matrix. The array manifold matrix $\mathbf{A}$ is orthogonal to $\mathbf{U}_N$ as $\mathbf{A}$ and $\mathbf{U}_S$ span the same subspace. On the other hand, there is a more efficient noise subspace projector $\prod_N \in \mathbb{H}_{\mathbb{C}}^{2(MN-L)\times 2(MN-L)}$ in the biquaternion model, and projector is $\prod_N = \sum_{p=2L+1}^{2(MN-L)} \mathbf{u}_p\mathbf{u}_p{}^{\dagger}$ that is built with the $2(MN-L)$ eigenvectors of $\mathbf{U}_N$. Therefore, the subspace orthogonality over biquaternion can be express as

$$\mathbf{a}^{\dagger}\prod_N = \mathbf{0}. \tag{27}$$

In practice, this equation does not strictly hold due to the finite number of snapshots and the presence of noise. We can construct the spectrum function of BQ-MUSIC as

$$\begin{aligned} F(\theta,\varphi,\gamma,\eta) &= \frac{1}{\det\left[\mathbf{a}^{\dagger}\prod_N\prod_N^{\dagger}\mathbf{a}\right]} \\ &= \frac{1}{\det\left[\xi^{\dagger}(\theta,\varphi,\gamma,\eta)\mathbf{q}(\theta,\varphi)\prod_N\prod_N^{\dagger}\mathbf{q}(\theta,\varphi)\xi(\theta,\varphi,\gamma,\eta)\right]}. \end{aligned} \tag{28}$$

As $0 \le \gamma \le \pi/2$, $\xi(\theta,\varphi,\gamma,\eta) \neq 0$ always holds. $\mathbf{q}(\theta,\varphi)\prod_N \prod_N^{\dagger}\mathbf{q}(\theta,\varphi)$ is full rank under the assumption of $L < MN$. Based on rank reduction principle, the spectrum function can be simplified from $F(\theta,\varphi,\gamma,\eta)$ to $F(\theta,\varphi)$, namely,

$$F(\theta,\varphi) = \frac{1}{\det\left[\mathbf{q}(\theta,\varphi)\prod_N\prod_N^{\dagger}\mathbf{q}(\theta,\varphi)\right]}. \tag{29}$$

And the final estimated value is

$$\left(\widehat{\theta},\widehat{\varphi}\right) = \arg\max_{\theta,\varphi}\frac{1}{\det\left[\mathbf{q}(\theta,\varphi)\prod_N\prod_N^{\dagger}\mathbf{q}(\theta,\varphi)\right]}. \tag{30}$$

The direction parameters $(\widehat{\theta},\widehat{\varphi})$ are obtained from $F(\theta,\varphi)$ through 2-D peak searching avoiding 4-D peak searching successfully. Our proposed BQ-MUSIC is summarized in Table 1.

Table 1: Summary of the proposed method.

Step 1: encode the received data to i, j, k and construct vector $\mathbf{X}(t)$
Step 2: calculate the covariance matrix $\mathbf{R}_X$ and perform biquaternion-valued EVD
Step 3: construct projector $\prod_N$ based on $\mathbf{U}_N$
Step 4: estimate the DOAs $\left(\widehat{\theta},\widehat{\varphi}\right)$ through 2-D peak searching in Eqs. (29) and (30)

Table 2: Calculation effort comparison.

	Memory size (real value)	Real multiplications	Real additions
LV-MUSIC	$18(MN)^2$	$4CM_{\mathrm{LV}}$	$3CM_{\mathrm{LV}}$
BQ-MUSIC	$8(MN)^2$	$4CM_{\mathrm{BQ}}$	$3CM_{\mathrm{BQ}}$

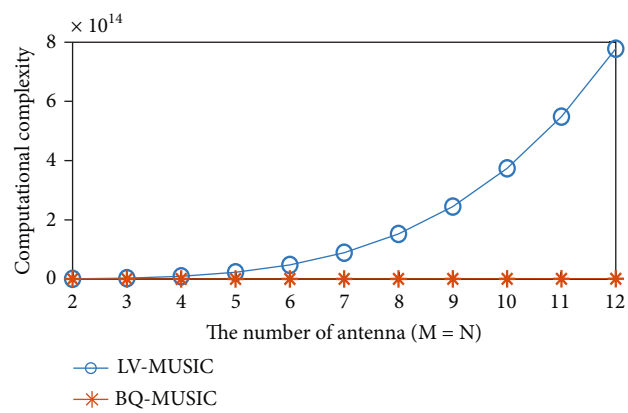

Figure 5: Computational complexity versus the number of antennas.

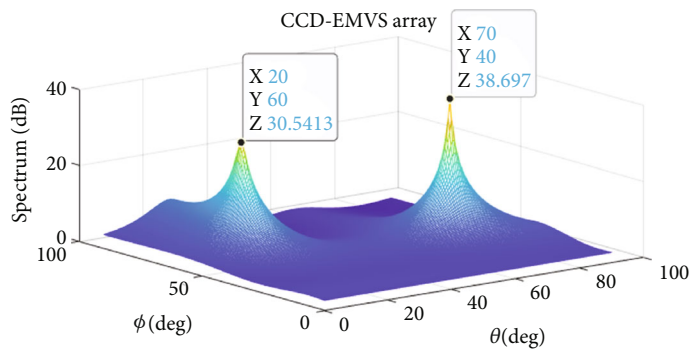

Figure 6: Spectrum of CCD-EMVS array.

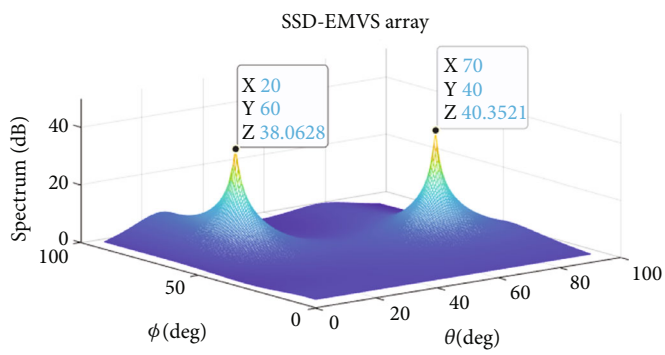

Figure 7: Spectrum of SSD-EMVS array.

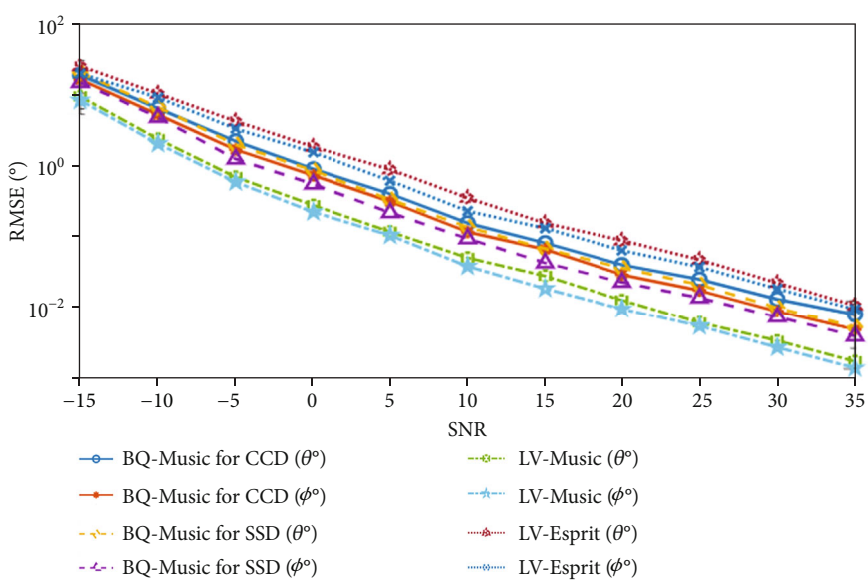

Figure 8: RMSE versus SNR.

5. Computational Analysis

Compared with the LV-model, the biquaternion model reduces the memory requirements of the covariance spectrum matrix by 4/9. And it is more valuable that the algorithm proposed in this paper simplifies the unapplicable 4-D peak search for $(\theta, \varphi, \gamma, \eta)$ to a 2-D search for (θ, φ), which greatly reduces the calculation burden.

The multiplication of two biquaternions implies 16 complex multiplications, and the addition of two biquaternions implies 4 complex additions. For the LV-MUSIC in Ref. [13], the received data matrix is $3MN \times K$, where K is the

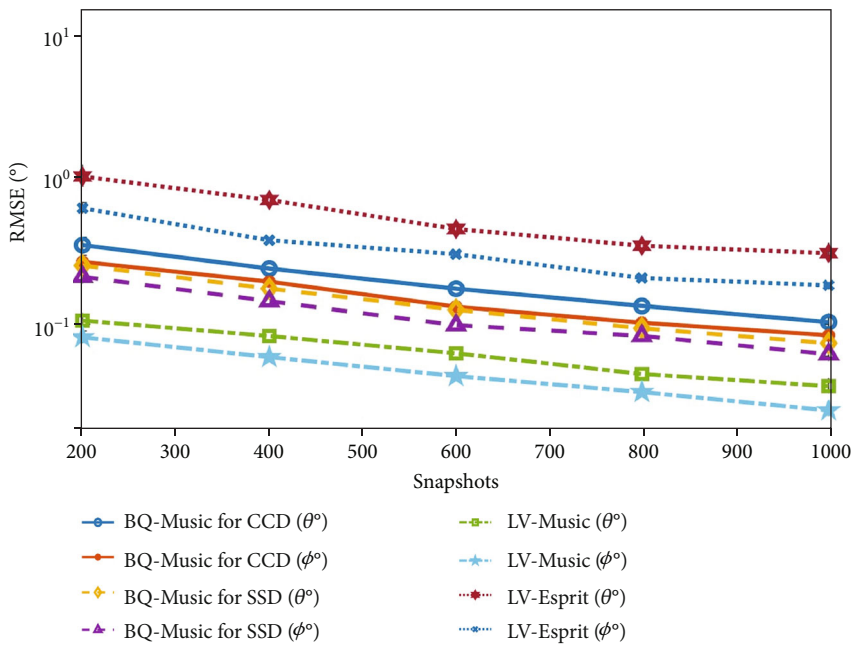

Figure 9: RMSE versus snapshots.

number of snapshots. The number of complex multiplications required to calculate the covariance matrix is $(3MN)^2 K$. The dimension of the covariance matrix is $3MN \times 3MN$, and calculating the EVD requires $(3MN)^3$ complex multiplications. The number of complex multiplications required to calculate the value of a spectrum function is $3MN[2(3MN - L) + 1]$. It is assumed that the search angle interval is Δ, and the LV-model requires $2\pi^4/\Delta^4$ searches. Finally, the total amount of complex multiplications required for LV-MUSIC is

$$CM_{\mathrm{LV}} = (3MN)^2 K + (3MN)^3 + 2(\pi/\Delta)^4 \times 3MN[2(3MN - L) + 1]. \tag{31}$$

For the BQ-MUSIC, the number of complex multiplications that requires to calculate the $MN \times K$ dimensional data matrix is $(9MN)^2 K$ since the multiplication of two pure biquaternions implies 9 complex multiplications. The EVD of biquaternion value matrix with the dimension of $MN \times MN$ is replaced by quaternion adjoint matrix with the dimension of $2MN \times 2MN$. Then the quaternion adjoint matrix is replaced by complex-value matrix with the dimension of $4MN \times 4MN$, and thus the complex multiplication of EVD is $(4MN)^3$. The complex multiplications required to create the projector matrix $\prod_{\mathrm{N}}$ is $16(MN)^2(MN - 2L)$. Calculation of the value of a spatial spectrum function requires $(16MN)^2 + (16MN)^2 + 16(MN)^2$ complex multiplications. The 2-D DOA search requires about $2\pi^2/\Delta^2$ searches. The total amount of complex multiplications required for BQ-MUSIC is

$$CM_{\mathrm{BQ}} = (9MN)^2 K + (4MN)^3 + (4MN)^2(MN - 2L) + \left(2\pi^2/\Delta^2\right)(MN)^2. \tag{32}$$

Since one complex multiplication operation contains four real multiplications and three real additions, the final computation and memory requirement space are compared in Table 2. A comparison of the computational complexity of the proposed algorithm and the LV-MUSIC algorithm is exhibited in Figure 5, where we set $\Delta = 1^\circ$. Let us evaluate the total number of arithmetic operations using complex multiplication as an indicator. The huge gap between the two is mainly reflected in 2-D search and 4-D search, because BQ-MUSIC can easily achieve dimensionality reduction. Moreover, as the search interval decreases, the difference in computational complexity between the two will further increase.

6. Simulation Results

In this section, we use numerical simulation experiments to verify the effectiveness of the proposed algorithm. In the following simulation, the size of the array is 4×4, with a total of 16 SSD-EMVS antennas, the distance $\mathrm{D}_x = \mathrm{D}_y = \lambda/2$ between adjacent antennas, and $d_x = d_y = d_z = d/10$. It is supposed that there are 2 independent targets $(L = 2)$, and their parameters are $\theta = (20^\circ, 70^\circ)$, $\varphi = (60^\circ, 40^\circ)$, $\gamma = (45^\circ, 75^\circ)$, and $\eta = (50^\circ, 35^\circ)$, respectively. Snapshots $K = 512$ and signal-to-noise ratio (SNR) are set as 10dB with the Gaussian white noise environment.

Simulation experiment: as shown in Figures 6 and 7, respectively, the spatial spectrum for CCD-EMVS array and SSD-EMVS array is obtained by BQ-MUSIC. It is obvious that both of them can accurately obtain the direction parameters. Furthermore, the spatial spectrum of SSD-EMVS has shaper peaks.

In Section 4, we conclude that the covariance matrix of the SSD-EMVS array is identical to the real part of the covariance matrix of the collocated type, with only a small

difference in the imaginary part. This difference is actually caused by the introduction of the spatial phase shift factor, because the spatial phase shift factor contains directional information. It ultimately leads to a better estimation of the SSD-EMVS array than the CCD-EMVS array by comparing Figures 6 and 7.

Performance analysis: we keep the above conditions unchanged, only change the SNR to perform 100 Monte-Carlo experiments, and define root mean squared error (RMSE) to measure the estimated performance, as

$$\mathrm{RMSE} = \sqrt{\frac{1}{L}\sum_{l=1}^{L} E\left[\left(\alpha\wedge_l - \alpha_l\right)^2\right]}, \tag{33}$$

where $\widehat{\alpha} = \{\widehat{\theta}, \widehat{\varphi}\}$ is 2-D parameter estimation, and $\alpha = \{\theta, \varphi\}(l = 1, 2)$ is the true value of parameter. As shown in Figure 8, the performance of the CCD-EMVS array is not as good as the SSD-EMVS array, which is in line with the above experimental results. Based on coarse-fine estimation, LV-ESPRIT [19] for SSD-EMVS array has poor performance with minimal computational complexity. The MUSIC algorithm is highly dependent on the matrix dimension, and the biquaternion model compresses the size of the vector to one-third of the long vector, which is the reason why the BQ-MUSIC algorithm is not as superior as the LV-MUSIC.

We assume that SNR = 10dB, the number of snapshots K is various, and other simulation conditions are constant. By plotting the RMSE variation curve with the number of snapshots, a similar conclusion to the previous simulation can be obtained from Figure 9.

7. Conclusion

A new MUSIC algorithm for SSD-EMVS array is proposed based on a biquaternion model. By illustrating the approximation of the CCD-EMVS array and the SSD-EMVS array covariance matrix, it is clear that the use of the subspace orthogonality property enables the SSD-EMVS array to obtain good DOA estimation performance. The dimensionality reduction algorithm of BQ-MUSIC makes it more practical than LV-MUSIC.

Data Availability

There is no available data for this study.

Conflicts of Interest

The authors declared that they have no conflicts of interests.

Acknowledgments

This work was supported by the Natural Science Foundation of Shaanxi Province under grant 2019-JM115.

References

[1] A. Nehorai and E. Paldi, "Vector-sensor array processing for electromagnetic source localization," *IEEE Transactions on Signal Processing*, vol. 42, no. 2, pp. 376–398, 1994.

[2] H. L. Van Trees, *Optimum Array Processing: Part IV of Detection, Estimation, and Modulation Theory*, John Wiley & Sons, New York, NY, USA, 2004.

[3] K. T. Wong and M. D. Zoltowski, "Self-initiating MUSIC-based direction finding and polarization estimation in spatio-polarizational beamspace," *IEEE Transactions on Antennas and Propagation*, vol. 48, no. 8, pp. 1235–1245, 2000.

[4] M. D. Zoltowski and K. T. Wong, "ESPRIT-based 2-D direction finding with a sparse uniform array of electromagnetic vector sensors," *IEEE Transactions on Signal Processing*, vol. 48, no. 8, pp. 2195–2204, 2000.

[5] D. Levin, E. A. Habets, and S. Gannot, "Maximum likelihood estimation of direction of arrival using an acoustic vector-sensor," *The Journal of the Acoustical Society of America*, vol. 131, no. 2, pp. 1240–1248, 2012.

[6] X. Yuan, "Polynomial-phase signal source tracking using an electromagnetic vector-sensor," in *2012 IEEE International Conference on Acoustics, Speech and Signal Processing (ICASSP)*, pp. 2577–2580, IEEE, 2012.

[7] G. Zheng, "A novel spatially spread electromagnetic vector sensor for high-accuracy 2-D DOA estimation," *Multidimensional Systems and Signal Processing*, vol. 28, no. 1, pp. 23–48, 2017.

[8] J. Tan and Z. Nie, "Polarization smoothing generalized MUSIC algorithm with polarization sensitive array for low angle estimation," *Sensors*, vol. 18, no. 5, article 1534, 2018.

[9] G. Zheng and B. Wu, "Polarisation smoothing for coherent source direction finding with multiple-input and multiple-output electromagnetic vector sensor array," *IET Signal Processing*, vol. 10, no. 8, pp. 873–879, 2016.

[10] S.-C. Pei, J.-H. Chang, and J.-J. Ding, "Commutative reduced biquaternions and their Fourier transform for signal and image processing applications," *IEEE Transactions on Signal Processing*, vol. 52, no. 7, pp. 2012–2031, 2004.

[11] N. Le Bihan and J. Mars, "Singular value decomposition of quaternion matrices: a new tool for vector- sensor signal processing," *Signal Processing*, vol. 84, no. 7, pp. 1177–1199, 2004.

[12] S. Miron, N. Le Bihan, and J. I. Mars, "Quaternion-MUSIC for vector-sensor array processing," *IEEE Transactions on Signal Processing*, vol. 54, no. 4, pp. 1218–1229, 2006.

[13] N. Le Bihan, S. Miron, and J. I. Mars, "MUSIC algorithm for vector-sensors array using biquaternions," *IEEE Transactions on Signal Processing*, vol. 55, no. 9, pp. 4523–4533, 2007.

[14] W. Si, T. Zhu, and M. Zhang, "Dimension-reduction MUSIC for jointly estimating DOA and polarization using plane polarized arrays," *Journal on Communications*, vol. 35, no. 12, pp. 28–35, 2014.

[15] J. Zhao, H. Tao, and National Laboratory of Radar Signal Processing, Xidian University, "Quaternion based joint DOA and polarization parameters estimation with stretched three-component electromagnetic vector sensor array," *Journal of Systems Engineering and Electronics*, vol. 28, no. 1, pp. 1–9, 2017.

[16] G. Wang, X. Wang, L. Wang, and X. Wang, "Research on ambiguity resolution algorithm by quaternion based on acoustic vector sensor," *Journal of Sensors*, vol. 2020, Article ID 2402489, 8 pages, 2020.

[17] H. Chen, W. Wang, and W. Liu, "Augmented quaternion ESPRIT-type DOA estimation with a crossed-dipole array," *IEEE Communications Letters*, vol. 24, no. 3, pp. 548–552, 2019.

[18] K. T. Wong and X. Yuan, ""Vector cross-product direction-finding" with an electromagnetic vector-sensor of six orthogonally oriented but spatially noncollocating dipoles/loops," *IEEE Transactions on Signal Processing*, vol. 59, no. 1, pp. 160–171, 2010.

[19] G. M. Zheng, B. X. Chen, and B. Wu, "DOA estimation with three orthogonally oriented and spatially spread polarization sensitive array," *Journal of Electronics & Information Technology*, vol. 36, no. 5, pp. 1088–1093, 2014.

[20] X. Gong, J. Jiang, H. Li, Y. Xu, and Z. Liu, "Spatially spread dipole/loop quint for vector-cross-product-based direction finding and polarisation estimation," *IET Signal Processing*, vol. 12, no. 5, pp. 636–642, 2018.